IN VIVO *39*: 1440-1452 (2025)
doi: 10.21873/invivo.13945

Effect of DNA Aptamer Concentration on the Stability of PDA Nanoparticle-based Electrochemical Biosensor to Detect Glycated Albumin

OHNMAR ZAW[1], NANG NOON SHEAN AYE[1], PAWEENA TUNAKHUN[1], JUREERUT DADUANG[1], SAKDA DADUANG[2] and PORNSUDA MARAMING[1]

[1]Centre for Research and Development of Medical Diagnostic Laboratories, Faculty of Associated Medical Sciences, Khon Kaen University, Khon Kaen, Thailand;
[2]Division of Pharmacognosy and Toxicology, Faculty of Pharmaceutical Sciences, Khon Kaen University, Khon Kaen, Thailand

Abstract

Background/Aim: The glycated albumin (GA), a potential biomarker for monitoring diabetes mellitus, reflects short-term glycemia and is not influenced by conditions that falsely alter hemoglobin A1c (HbA1c) levels. This study presents a comprehensive evaluation of DNA aptamer-functionalized polydopamine nanoparticles (PDA NPs) for developing a stable biosensor targeting GA.

Materials and Methods: DNA aptamers, conjugated to PDA NPs at varying aptamer concentrations (0.05, 0.5, and 5 μM), were systematically analyzed to understand their impact on the morphological, electrochemical behavior, and stable responses of the biosensor.

Results: Morphological assessments using transmission electron microscopy, scanning electron microscopy, and atomic force microscopy confirmed the stability of PDA NPs after conjugation with aptamers. Electrochemical characterization demonstrated enhanced electron transfer efficiency at an optimal aptamer concentration (0.5 μM) for GA detection while stability testing over 30 days indicated sustained sensor functionality.

Conclusion: The PDA-0.5 μM aptamer conjugations balance structural integrity, and stability, emphasizing the importance of aptamer concentration optimization for practical biosensor applications.

Keywords: Polydopamine nanoparticles, DNA aptamer, aptamer-functionalized nanoparticles, electrochemical biosensor, stability testing, glycated albumin.

Pornsuda Maraming, Ph.D., Assistant Professor, Faculty of Associated Medical Sciences, Khon Kaen University, 123 Mittraphap Road, Muang Khon Kaen, Khon Kaen 40002, Thailand. Tel: +66 0825936726, e-mail: pornsma@kku.ac.th

Received February 4, 2025 | Revised February 22, 2025 | Accepted February 25, 2025

Introduction

Diabetes mellitus is a widespread health concern defined by prolonged high blood-sugar levels caused by either a lack of insulin or resistance to its effects (1). Glycated albumin (GA) is an important biomarker for assessing medium-term glucose control, complementing short-term measures like glucose level and long-term indicators such as hemoglobin A1c (HbA1c) (2). GA concentration provides valuable information about blood-sugar variability, especially in individuals experiencing rapid fluctuations or conditions that affect hemoglobin metabolism (3). The precise and consistent detection of GA is crucial for tailored diabetes care, highlighting the importance of advanced and reliable biosensor technologies.

Functionalizing nanoparticles with DNA aptamers has become a prominent approach in developing highly sensitive and specific biosensors (4-6). DNA aptamers are highly specific, high-affinity oligonucleotides that outperform traditional recognition elements like antibodies (7-11). Their advantages include easy synthesis, stability under harsh conditions, and high selectivity. DNA aptamers conjugated to polydopamine nanoparticles (PDA NPs) enhance biosensor applications due to the properties of polydopamine relating to biocompatibility, adhesiveness, and versatile bonding (12-15). Thus, PDA is ideal for stable biosensors, especially for detecting GA in diabetes management.

PDA, inspired by the adhesive properties of mussel foot proteins, presents both amine and catechol groups on its surface, enabling easy functionalization with a variety of molecules, including DNA aptamers, *via* covalent and non-covalent interactions (16-18). These interactions contribute to the stability of the aptamers on the PDA surface, preventing desorption and ensuring that their bioactivity is preserved under biologically relevant conditions (19, 20). Several studies have demonstrated that the PDA NP-aptamer conjugation enhances biosensor performance by maintaining aptamer functionality over extended periods (21-25). For example, Cohen *et al.* (2021) reported that PDA-aptamer conjugates improved the long-term stability and reproducibility of glucose biosensors (25), while Xu *et al.* (2020) showed that the incorporation of PDA enhanced the specificity of aptamers in detecting cancer biomarkers (26). However, while PDA provides a robust platform, optimizing its functionalization with aptamers is crucial for achieving the best sensor performance.

DNA aptamers are synthetic oligonucleotides selected for their high specificity and affinity toward target molecules, offering advantages over antibodies due to their stability and ease of synthesis and modification (27, 28). Aptamers can form unique three-dimensional structures that enable selective recognition of biomarkers, such as GA (29, 30). When conjugated to PDA NPs, these aptamers can retain their structural conformation, enabling high target selectivity even in the presence of interfering molecules (31). This makes aptamer-functionalized PDA NPs a promising platform for sensitive, stable, and efficient biosensors.

The concentration of DNA aptamers on the PDA surface plays a critical role in determining the performance of the resulting biosensor (32). Several studies have addressed the impact of aptamer concentration on sensor sensitivity and stability (33, 34). For instance, White *et al*. (2008) demonstrated that increasing aptamer density improved the sensor's sensitivity to target molecules (33). However, excessive aptamer concentration led to steric hindrance, which impaired electron-transfer efficiency. Similarly, Hu *et al.* (2023) found that a lower aptamer concentration on PDA surfaces reduced binding sites, diminishing sensor sensitivity (34). These findings underscore the importance of optimizing aptamer concentration to balance the sensor's sensitivity and stability. However, as the aptamer concentration increases, issues such as aggregation, non-specific binding, and reduced stability may arise, potentially compromising the sensor's performance (35).

Despite the promising advantages of PDA NP-aptamer conjugates, several limitations exist that can hinder the practical application of these biosensors. One limitation is the potential for non-specific binding due to the adhesive nature of PDA, which could lead to a decrease in biosensor

specificity (36). Additionally, aptamers may aggregate at high concentrations resulting in the loss of aptamer flexibility and binding efficiency, which can decrease the overall performance of the biosensor (37). Furthermore, while PDA is biocompatible, the stability of the PDA NP-aptamer conjugates can be influenced by environmental factors such as pH, ionic strength, and temperature (38). These limitations highlight the need for further optimization in the functionalization process to ensure the consistent performance of PDA NP-aptamer based biosensors.

This study evaluates the effects of different DNA aptamer concentrations (0.05, 0.5, and 5 μM) on the morphology, electrochemical properties, and stability of PDA-aptamer conjugates for designing an optimized PDA-based biosensor. Surface morphology and structural integrity were analyzed using transmission electron microscopy (TEM), scanning electron microscopy (SEM), and atomic force microscopy (AFM). Electrochemical measurements were performed to investigate the effect of scan rate on the electrochemical response and to evaluate the detection of GA using a PDA NP-aptamer-based electrochemical biosensor at different aptamer concentrations. A 30-day stability test examined long-term functionality. Results identified the optimal aptamer concentration for maximizing stability, and electrochemical measurements, contributing to advances in GA detection. The insights gained from this study are anticipated to have broad implications for the development of next-generation biosensors that prioritize stability, and adaptability, paving the way for more effective and accessible diagnostic tools in the future.

Materials and Methods

Materials. All chemicals and reagents used in this study were of analytical grade. Dopamine hydrochloride (MW=189.6), and ethanolamine were purchased from Sigma-Aldrich (St. Louis, MO, USA). Tris base (MW=121.14) was obtained from Promega Corporation (Madison, WI, USA). An amine-modified aptamer with a 23-base sequence, 5'-NH_2-TGC GGT TGT AGT ACT CGT GGC CG-3' (39), was custom-synthesized by Integrated DNA Technologies Pte. Ltd., Singapore Science Park II, Singapore. Screen-printed carbon electrodes (SPCEs) were obtained from Quasense (Bangkok, Thailand). Deionized water (DI water) was used for rinsing steps.

Instruments and apparatus. Electrochemical measurements, including cyclic voltammetry (CV) and differential pulse voltammetry (DPV), were conducted using a PalmSens4 potentiostat system (PalmSens BV Co., Ltd., Utrecht, the Netherlands) with PS trace 5.6 software. A three-electrode system comprising a silver/silver chloride (Ag/AgCl) reference electrode, a 2.5 mm diameter carbon working electrode, and a carbon counter electrode was employed. The morphological characteristics of the PDA NPs, including structure and surface topography, were assessed using transmission electron microscopy (TEM, FEI, TECNAI G2 20, Thermo Fisher Scientific, Waltham, MA, USA), scanning electron microscopy (SEM, FEI, Helios NanoLab G3 CX, Thermo Fisher Scientific) and atomic force microscopy (AFM, XE-120, Park System Corporation, Suwon, Gyeonggi-do, Republic of Korea) to investigate both the PDA NPs and the PDA NP-aptamer conjugates. The size and polydispersity index (PDI) measurements of the PDA NPs and PDA NP-aptamer conjugates were measured by a Zetasizer Nano ZS instrument (Malvern Panalytical, Malvern, Worcestershire, UK). A redox indicator was prepared using 5 mM potassium ferricyanide ($K_3[Fe(CN)_6]$) in 0.1 M potassium chloride (KCl) with phosphate-buffered saline (PBS) (1X, pH 7.4).

Preparation of PDA NP-aptamer conjugates on SPCEs. PDA NPs were synthesized and PDA NP-aptamer-modified SPCEs were made. To prepare PDA NPs, dopamine hydrochloride (0.5 mg ml^{-1}) was dissolved in 10 mM Tris buffer (pH 10.5) and stirred for 20 h at room temperature. The nanoparticles were then centrifuged at 16,100×*g* and washed twice with Tris buffer to remove unreacted dopamine. To fabricate PDA NPs/aptamer/ethanolamine-modified SPCEs, the purified PDA NPs were then functionalized with DNA aptamers at three concentrations (0.05, 0.5, and 5 μM). The mixture was incubated at room

temperature for 45 min to enable the amine-catechol interaction between PDA NPs and aptamer amine groups. Seven μl of the conjugates were deposited on the working carbon electrode and incubated for 30 min, followed by washing with PBS (0.01 M, pH 7.4). To minimize non-specific binding, the PDA NP-aptamer conjugates were treated with ethanolamine. Following immobilization, the particles were incubated with ethanolamine (0.1 M) solution for 30 min to block any remaining reactive sites on the PDA surface. This step was followed by washing with DI water to remove excess ethanolamine.

TEM study. TEM was used to examine the morphology of PDA NPs and PDA NP-aptamer conjugates. For TEM imaging, a 20 μl drop of each PDA NP-aptamer suspension was placed onto a carbon-coated copper grid and allowed to air dry, forming a uniform, thin film on the grid surface. This preparation enabled clear visualization of the PDA NPs before and after aptamer conjugation, providing insights into any structural changes associated with different aptamer concentrations.

SEM study. SEM was utilized to examine the surface morphology of PDA NPs and PDA NP-aptamer conjugates at various aptamer concentrations. For SEM sample preparation, a 7 μl drop of each conjugate suspension was carefully applied onto a SPCE and allowed to air dry, creating a stable, uniform film on the electrode surface for imaging. SEM images were captured at an accelerating voltage of 10 kV to visualize morphological differences between bare PDA NPs and PDA NP-aptamer conjugates at different concentrations, providing insights into the effect of aptamer loading on nanoparticle structure and surface features.

AFM study. AFM was used to measure the surface topography of bare SPCE, SPCEs coated with PDA NPs, and SPCEs coated with PDA NP-aptamer conjugates at various aptamer concentrations. Seven μl of each sample were deposited on SPCEs and allowed to dry. Imaging was conducted in tapping mode with a silicon cantilever. The AFM data, scanned at 256×256 pixels resolution over 10 μm×10 μm areas at 0.5 Hz, were analyzed for surface roughness and structural changes attributed to varying aptamer concentrations. XEI software (Park System Corporation) was used for image processing and quantitative analysis.

Electrochemical measurements for scan rate study. Electrochemical studies were performed to assess the impact of aptamer concentration on the electron transfer properties of the SPCEs modified with PDA NP-aptamer conjugates. Each SPCE was modified by depositing 7 μl of the PDA NP-aptamer suspension and allowing it to dry. CV was conducted using a potentiostat with 5 mM $K_3[Fe(CN)_6]$ and 0.1 M KCl in PBS (1X, pH 7.4). Scan rates varied from 10 to 300 mVs^{-1}, and CV responses were recorded. The data were analyzed to determine the peak current and electron transfer rate for each concentration, providing insights into how aptamer concentration affects electrochemical performance.

Electrochemical measurements for GA detection. Electrochemical measurements were conducted to evaluate the performance of the PDA NP-aptamer modified electrodes for GA detection. PDA NP/aptamer/ethanolamine-modified SPCEs were fabricated by conjugating PDA NPs with varying aptamer concentrations (0.05, 0.5, and 5 μM) for 45 min. Seven μL of the conjugates were drop-coated onto SPCEs and incubated for 30 min. After washing with PBS, 0.1 M ethanolamine was used for 30 min to block non-specific binding. Following another PBS wash, the modified electrodes were exposed to a 1000 $\mu g\ ml^{-1}$ solution of GA, and incubated for 60 min to ensure binding. Following this step, a redox indicator was introduced to the electrode system, and DPV was conducted from −0.015 to 0.6 V at 100 mVs^{-1} to monitor the electrochemical response. The peak current corresponding to the redox activity of the GA was analyzed to quantify the binding interactions and evaluate the sensor's performance. The flow diagram of the proposed electrochemical aptasensor is illustrated in Figure 1.

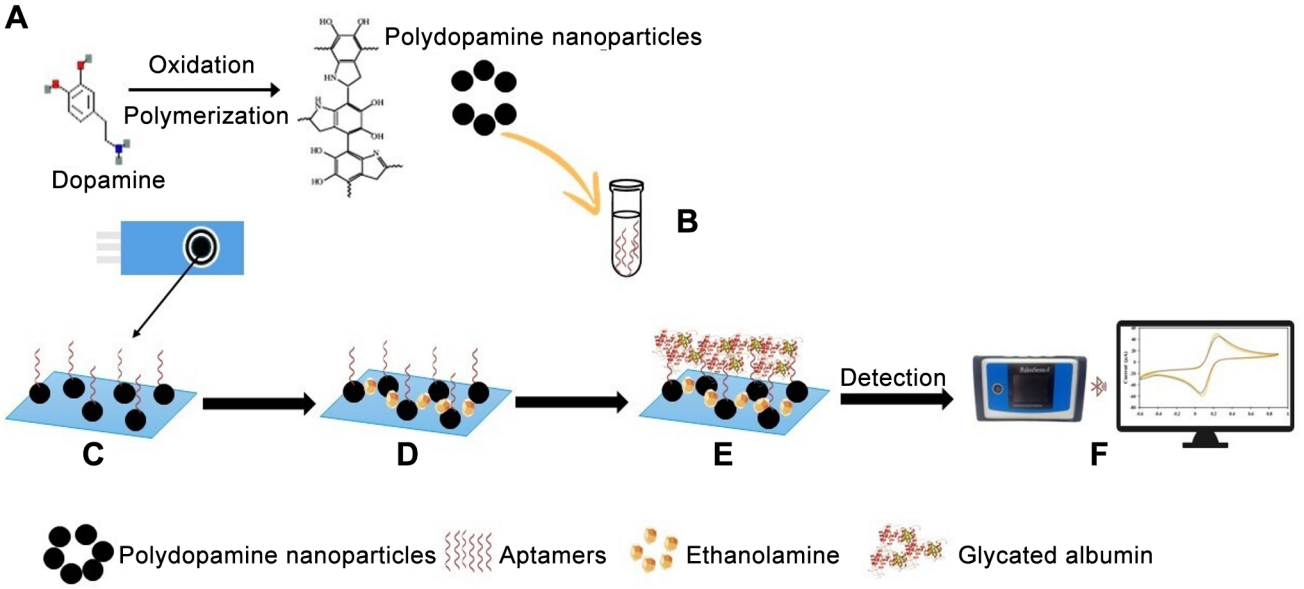

Figure 1. *Schematic diagram of the proposed polydopamine nanoparticle (PDA NP) functionalized electrochemical aptasensor for detection of glycated albumin (GA). (A) Synthesis of PDA NPs, (B) conjugation of aptamer- NH_2 to PDA NPs, (C) drop coating PDA NPs functionalized with aptamer onto screen-printed carbon electrodes (SPCEs), (D) blocking with ethanolamine, (E) incubation with GA and (F) voltammetric measurements using 5 mM $[Fe(CN)_6]^{4-/3-}$ as a redox indicator.*

Stability testing. The stability of PDA NP-aptamer conjugates on SPCEs was evaluated over a 30-day period. Each sensor was stored at room temperature and tested at intervals of 0, 7, 14, 21, and 30 days. The three aptamer concentrations used were 0.05, 0.5, and 5 µM. At each time point, the electrochemical response of each sensor was recorded using DPV, and the current response was calculated as a percentage of the initial response (day 0). Comparisons were made across the three aptamer concentrations to assess the influence of aptamer loading on sensor longevity.

Results

TEM, SEM and DLS studies. The images of TEM (Figure 2A-D) and SEM (Figure 3A-D) reveal the detailed morphology of PDA NPs and their modification at varying DNA aptamer concentrations 0.05, 0.5, and 5 µM. The initial, unmodified PDA NPs (Figure 2A) exhibited a spherical morphology with uniform size, averaging around 200 nm in diameter. The well-dispersed state of these nanoparticles suggests the favorable colloidal stability in aqueous media. Following functionalization with DNA aptamers at concentrations of 0.05, 0.5, and 5 µM, TEM images (Figure 2B-D) showed that the overall morphology and size of the PDA NPs remained relatively unchanged. Subsequently, SEM analyses indicated that the conjugation of PDA NPs with varying aptamer concentrations (0.05, 0.5, and 5 µM) had minimal impact on the overall size and surface morphology of the nanoparticles (Figure 3B-D) compared to unmodified PDA NPs (Figure 3A). The results obtained from a Zetasizer show that the particle size of PDA NPs increased from 153.37±0.61 nm with a narrow PDI to 319.0±53.95 nm upon aptamer conjugation. Higher aptamer concentrations led to larger particle sizes and higher PDI values, indicating increased surface modification (Table I).

AFM study. The AFM images in Figure 4 illustrate the 3D surface topography changes of SPCEs modified with PDA NPs with different aptamer concentrations. The average surface roughness (R_a) and root mean square surface roughness (R_q)

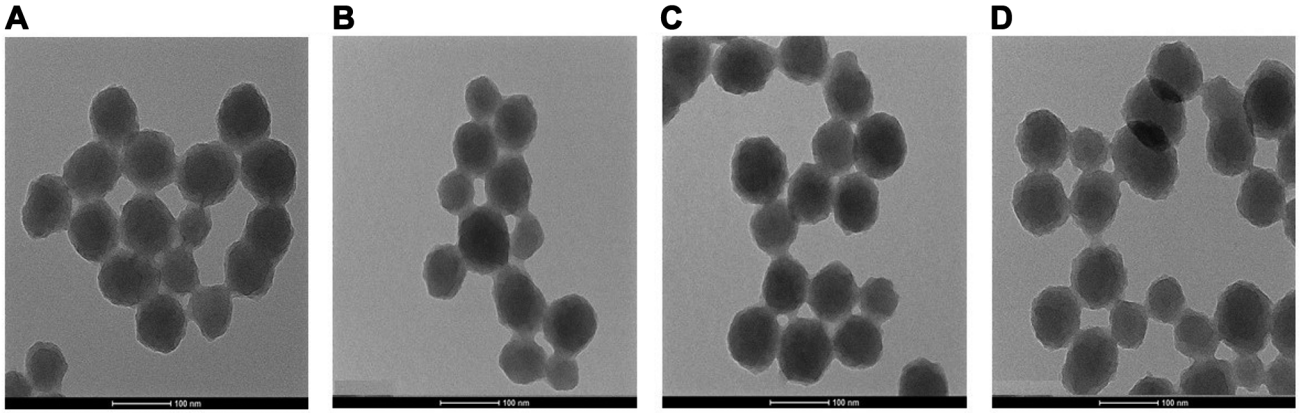

Figure 2. *Transmission electron microscopy (TEM) images of (A) polydopamine nanoparticles (PDA NPs), and PDA NPs conjugated with aptamer concentrations at (B) 0.05 μM, (C) 0.5 μM, (D) 5 μM.*

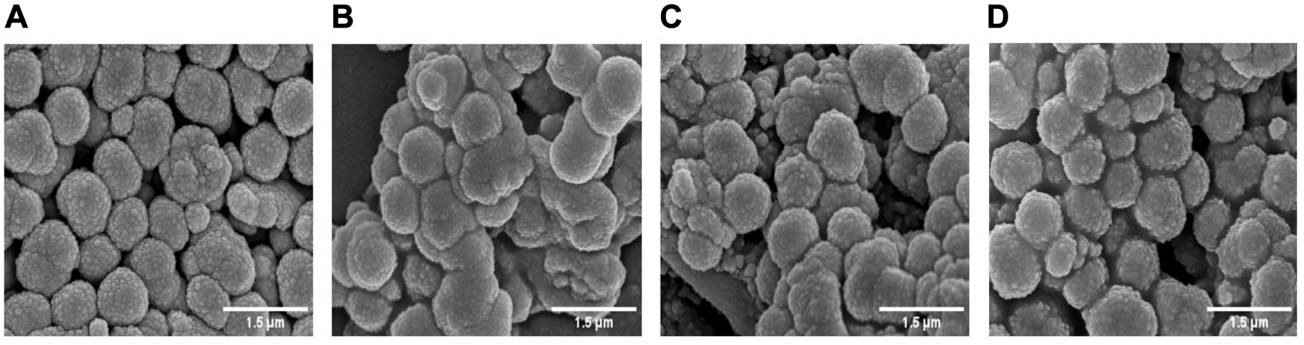

Figure 3. *Scanning electron microscopy (SEM) images of (A) polydopamine nanoparticles (PDA NPs) and PDA NPs conjugated with different aptamer concentrations (B) 0.05 μM, (C) 0.5 μM, (D) 5 μM.*

are summarized in Table II. The bare SPCE (Figure 4A) displayed R_a and R_q values of 0.16±0.1 μm and 0.21±0.12 μm, respectively. The SPCE modified with PDA NPs showed minimal changes in surface roughness (Figure 4B). After modification with different aptamer concentrations (Figure 4C-E), higher surface roughness was observed compared to bare SPCE and PDA NPs (Figure 4A-B). Table II demonstrates that increasing aptamer concentrations on PDA-modified SPCEs significantly enhanced surface roughness, indicating improved aptamer binding, denser surface coverage, and concordance with the AFM images.

Scan rate study. The scan rate-dependent CV analysis provided insights into the electrochemical behavior of bare SPCEs and SPCEs modified with PDA NP-aptamer conjugates functionalized with aptamer concentrations of 0.05, 0.5, and 5 μM. Figure 5A-D illustrates the CV profiles obtained at varying scan rates, whereas Figure 5E-H demonstrate the linear relationships between the peak current (I_{pa} and I_{pc})

Table I. *The size and polydispersity index (PDI) measurement of polydopamine nanoparticles (PDA NPs) and PDA NP-aptamer conjugates.*

Sample	Particle size (nm)	PDI
Bare PDA NPs	153.37±0.61	0.01±0.00
PDA NPs+0.05 μM aptamer	213.10±2.92	0.28±0.03
PDA NPs+0.5 μM aptamer	226.73±3.66	0.29±0.03
PDA NPs+5 μM aptamer	319.0±53.95	0.42±0.03

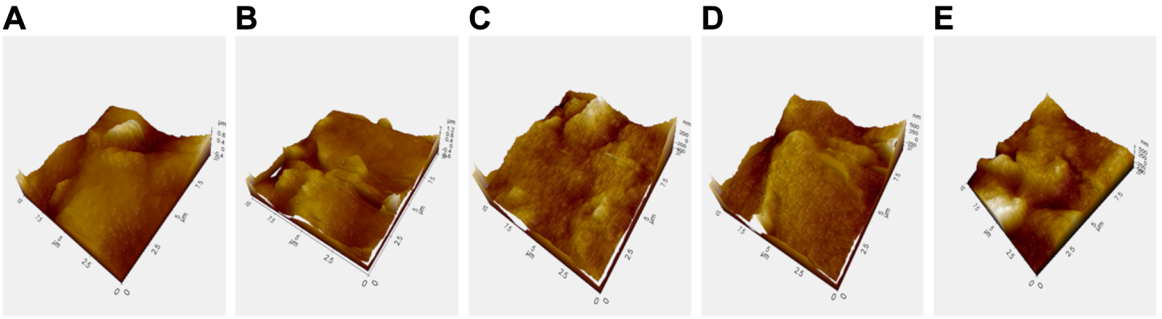

Figure 4. *Three-dimensional atomic force microscopy (AFM) microscale surface images of (A) bare screen-printed carbon electrode (SPCE), (B) SPCE modified with polydopamine nanoparticles (PDA NPs), and SPCEs modified with PDA NP-aptamer conjugates at different aptamer concentrations (C) 0.05, (D) 0.5, (E) 5 µM.*

Table II. *Evaluation of surface parameters using atomic force microscopy micrographs obtained from a 10×10 µm scan size.*

Parameter analysis	Bare SPCE	PDA NPs/SPCE	PDA NP-aptamer/SPCE at different aptamer concentrations (µM)		
			0.05	0.5	5
R_a (µm)	0.16±0.10	0.22±0.18	86.95±29.43	137.38±31.48	159.73±31.22
R_q (µm)	0.21±0.12	0.26±0.2	113.24±34.22	171.14±35.33	203.29±37.95

SPCEs: Screen-printed carbon electrodes; PDA: polydopamine; NPs: nanoparticles.

and the square root of the scan rate. These linear dependencies confirm that the electron transfer process is diffusion-controlled across all electrode configurations. The R^2 values for the linear regression analysis of peak current *versus* the square root of the scan rate were 0.9987 for bare SPCE, and 0.9985, 0.9995, and 0.9987 for SPCEs modified with PDA NP-aptamer conjugates at 0.05, 0.5, and 5 µM aptamer concentrations, respectively. The 0.5 µM aptamer-modified SPCE exhibited the highest correlation, indicating consistent diffusion-controlled behavior and optimal conditions for electrochemical performance.

Electrochemical measurements for GA detection. The biosensors for GA detection were tested using DPV at aptamer concentrations of 0.05, 0.5, and 5 µM, as shown in Figure 6A, which displays the DPV curves for bare SPCE, PDA NP-aptamer/SPCE, and GA/PDA NP-aptamer/SPCE. The results demonstrate a progressive decrease in peak current upon aptamer immobilization and subsequent GA binding. This decline is attributed to the hindrance of electron transfer caused by the PDA NP-aptamer coating and further reduction upon GA binding, indicating effective immobilization and high affinity between GA and the aptamer.

The peak current changes (ΔI) observed by the GA/PDA NP-aptamer/SPCE at different aptamer concentrations are presented in Figure 6B. The biosensor exhibited the highest current response with a minimal error bar at 0.5 µM aptamer concentration (3 replicates), suggesting optimal aptamer coverage and binding activity. At lower aptamer concentrations, a reduction in ΔI was observed, which can be attributed to a lower number of binding sites on the sensor surface, leading to decreased sensor performance. High aptamer concentrations likely caused steric hindrance due to excessive surface coverage, which restricted target molecules from accessing binding sites and reduced ΔI.

Stability testing. Figure 7 presents the stability of PDA NP-aptamer conjugate biosensors over 30 days that were

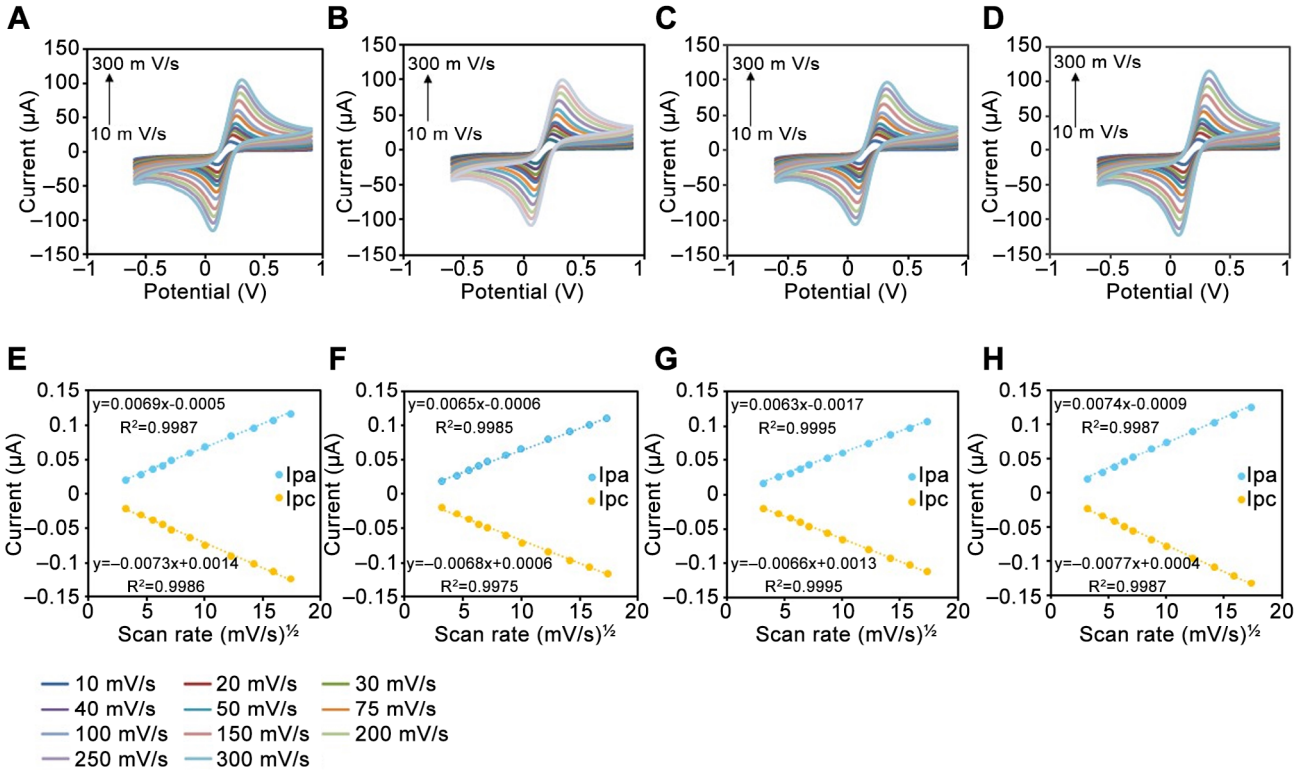

Figure 5. *Scan rate studies of cyclic voltammetry (CV) response. (A), (B), (C) and (D) CV obtained for different scan rates (10-300 mV/s), (E), (F), (G) and (H) the calibration plots of anodic peak current versus scan rate (10-300 mV/s) for different electrodes of bare screen printed carbon electrode (SPCE) and polydopamine nanoparticle (PDA NP)-aptamer/SPCE at different aptamer concentrations (0.05, 0.5, and 5 μM), respectively.*

evaluated across three aptamer concentrations: 0.05, 0.5, and 5 μM. Stability was quantified by measuring the current response to GA. At 0.05 μM, the biosensor exhibited a significant drop in current response, retaining less than 85% of its initial response by day 14, due to insufficient aptamer density and weak binding interactions. This instability limited its long-term performance. In contrast, the 0.5 μM concentration demonstrated excellent stability, maintaining over 90% of its initial current response for 30 days. The optimal aptamer coverage at this concentration ensured stable binding interactions and minimized desorption, supporting the biosensor's long-term structural integrity and reliability for sustained applications. At 5 μM, the biosensor exhibited a moderate decline in stability over time, retaining approximately 85% of its initial current response by day 30. Although the initial performance at this concentration was stable, the excessive aptamer coverage might lead to steric hindrance and aggregation, slightly impairing the electron transfer and the stability of binding interactions. This suggests that densely packed aptamers at 5 μM can hinder long-term functionality.

Discussion

The primary objective of this study was to optimize the aptamer concentration in PDA NP-aptamer conjugates modified on SPCEs for GA detection, aiming to achieve a balance between electrochemical efficiency and long-term stability. The findings suggest that an aptamer concentration of 0.5 μM provides the optimal condition for both properties.

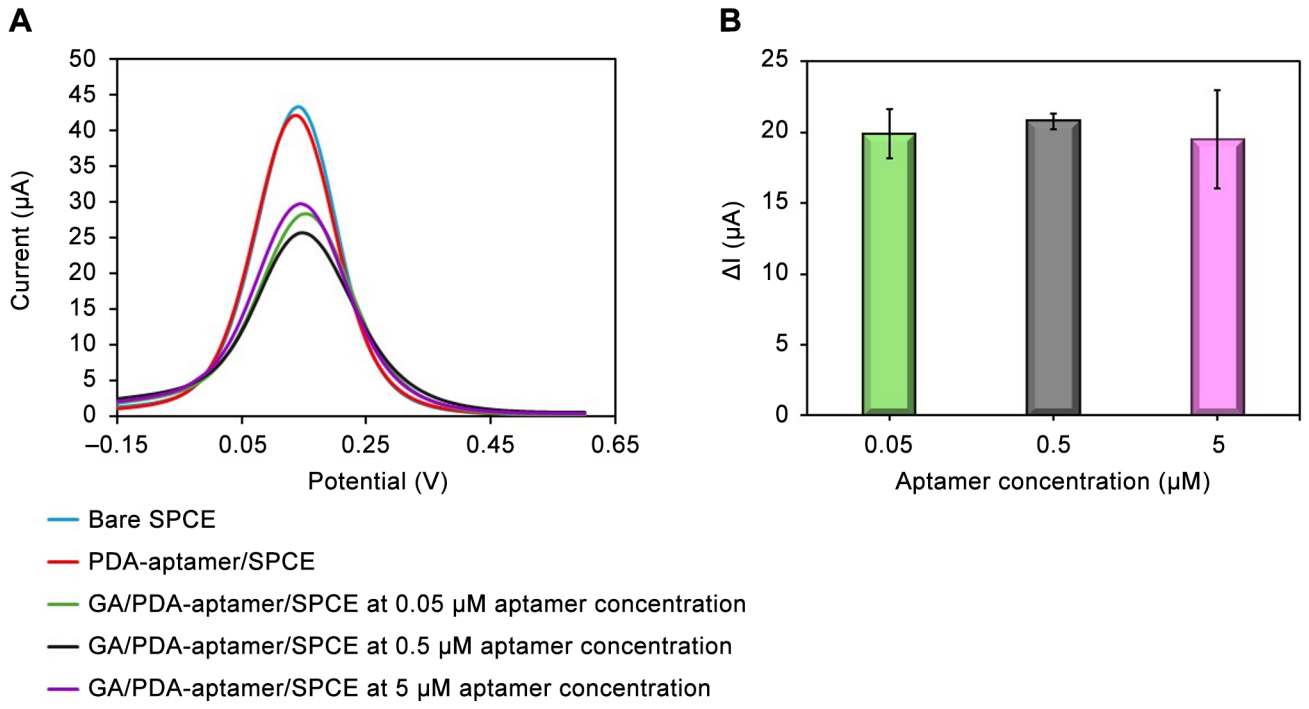

Figure 6. *Electrochemical measurements of glycated albumin (GA) detection. (A) Differential pulse voltammetry (DPV) curves for bare screen-printed carbon electrode (SPCE), polydopamine nanoparticle (PDA NP)-aptamer/SPCE, and GA/PDA NP-aptamer/SPCE and (B) bar graph illustrating the peak current change (ΔI) observed by the proposed biosensor at different aptamer concentrations (0.05, 0.5, and 5 μM).*

The relationship between aptamer concentration and sensor performance has been widely discussed in the literature (40-42). Our study supports the notion that both low (0.05 μM) and high (5 μM) aptamer concentrations have their drawbacks. At lower concentrations, the coverage of PDA NPs by aptamers is insufficient, which can lead to weaker molecular interactions and reduced sensor sensitivity. However, higher concentrations, while providing dense aptamer coverage, can result in steric effects that hinder efficient electron transfer and may reduce binding efficiency. This is consistent with a prior study, where excessive aptamer loading was shown to affect both the electrochemical behavior and the stability of aptamer-functionalized sensors (43).

The 0.5 μM concentration, as observed in this study, seems to strike the optimal balance and provide enough binding sites for target molecules. This intermediate concentration appears to promote effective electrochemical performance while maintaining the stability of the sensor over time. Table III shows the comparison of stability duration of aptasensors at different aptamer concentrations for GA detection. This study explored the highest stability of electrochemical based aptasensors for GA detection compared to previous studies (44-46).

The effects of complex biological samples on sensor performance warrant further investigation. In this study, the biosensor was evaluated in controlled buffer solutions; however, in actual clinical settings, sensors will need to perform reliably in more complex matrices, such as blood serum or plasma. The presence of proteins, salts, and other biomolecules could interfere with the sensor's performance. Future studies should assess the robustness of the PDA NP-aptamer conjugate biosensors in the presence of such interfering substances, ensuring its applicability in real-world diagnostic environments.

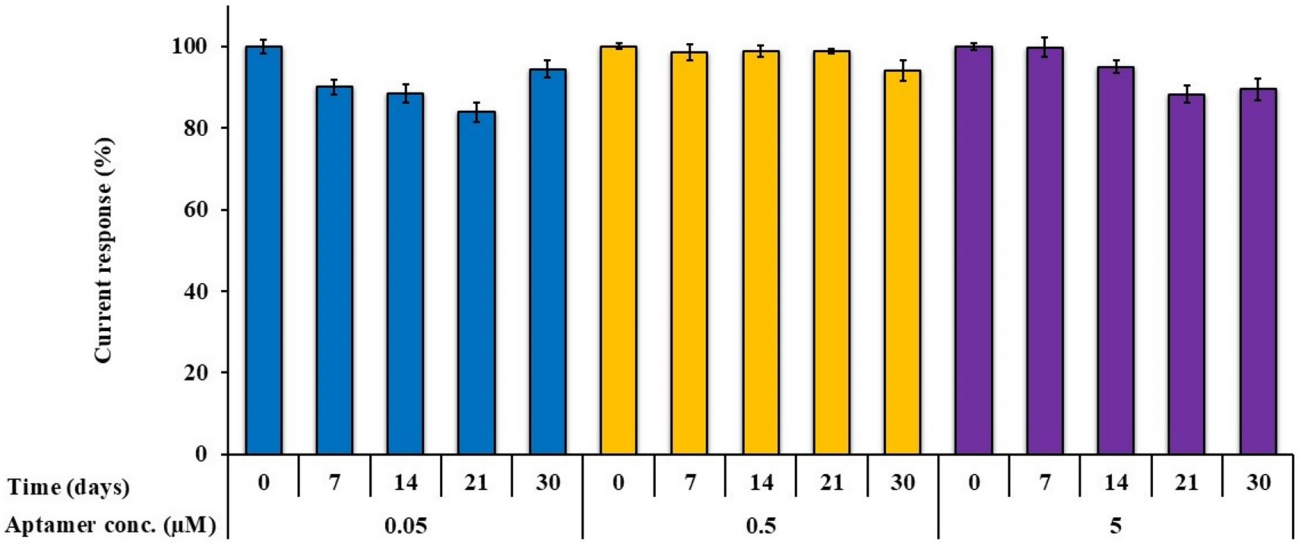

Figure 7. *Stability of aptasensors at three different aptamer concentrations (0.05, 0.5, and 5 µM) for 0, 7, 14, 21, and 30 days.*

Table III. *Comparison of stability durations of electrochemical based aptasensors for GA detection.*

Type of aptasensor	Aptamer sequence	Aptamer concentration	Current response (%) after 30 days	Ref.
BElectrochemical GO-aptasensor	5' -NH_2-TGC GGT TGT AGT ACT CGT GGC CG-3'	1 µM	84%	(44)
Electrochemical GO-aptasensor	5′-TGCGGTTCGTGCGGTTGTAGTAC-3′	2 µM	60%	(45)
Electrochemical aptasensor	5'-TGCGGTTGTAGTACTCGTGGCCG-3' (5del11 & 3del15)	1 µM	87%	(46)
Electrochemical PDA NP-aptasensor	5'-NH_2-TGC GGT TGT AGT ACT CGT GGC CG-3'	0.5 µM	94%	This work

Another avenue for future work lies in exploring the use of nanomaterials, such as gold nanoparticles or carbon nanotubes, in combination with PDA NP-aptamer conjugates. These materials have been shown to enhance the electrical conductivity of biosensors, which could further improve the sensitivity and speed of detection. Integrating these materials with PDA NP-based sensors might lead to even more efficient and reliable biosensors for biomarker detection.

Conclusion

These findings underscore the importance of aptamer concentration in optimizing biosensor stability. At 0.5 µM aptamer concentration, the proposed PDA NP-aptamer-based biosensor is achieving the optimal balance of surface coverage, binding stability, and structural durability. This concentration can be used in future studies to provide essential insights for developing stable, high-performance

aptamer-based biosensors for reliable GA detection. However, future research should focus on expanding the sensor's applicability, improving selectivity, and optimizing its performance in complex biological samples to meet the demands of real-world diagnostic applications.

Funding

This research was supported by the Fundamental Fund of Khon Kaen University, the National Science, Research, and Innovation Fund (NSRF). This study was also supported by the Centre of Research and Development of Medical Diagnostic Laboratories (CMDL), Faculty of Associated Medical Sciences, Khon Kaen University and Khon Kaen University ASEAN-GMS scholarship.

Conflicts of Interest

The Authors declare that the research was conducted in the absence of any commercial or financial relationships that could be construed as potential conflicts of interest.

Authors' Contributions

OZ: conceptualization, investigation, formal analysis, and writing–original draft. NNSA: methodology, writing–review, and editing. PT and SD: data curation, formal analysis, writing–review, and editing. JD: funding acquisition, writing–review, and editing. PM: conceptualization, methodology, supervision, funding acquisition, writing–review, and editing.

Acknowledgements

The Authors gratefully acknowledge the support received from the Centre of Research and Development of Medical Diagnostic Laboratories (CMDL), Faculty of Associated Medical Sciences, Khon Kaen University. The Authors would also like to express gratitude to Khon Kaen University for ASEAN and GMS countries' personnel for the academic year 2022. Furthermore, the authors would like to acknowledge Professor David Blair and the KKU publication clinic for editing the manuscript and providing insightful comments.

References

1 Antar SA, Ashour NA, Sharaky M, Khattab M, Ashour NA, Zaid RT, Roh EJ, Elkamhawy A, Al-Karmalawy AA: Diabetes mellitus: Classification, mediators, and complications; A gate to identify potential targets for the development of new effective treatments. Biomed Pharmacother 168: 115734, 2023. DOI: 10.1016/j.biopha.2023.115734

2 Roohk HV, Zaidi AR: A review of glycated albumin as an intermediate glycation index for controlling diabetes. J Diabetes Sci Technol 2(6): 1114-1121, 2008. DOI: 10.1177/193229680800200620

3 Dai D, Mo Y, Zhou J: Glycated albumin and its variability: Clinical significance, research progress and overall review. Obes Med 19: 100256, 2020. DOI: 10.1016/j.obmed.2020.100256

4 Chiu TC, Huang CC: Aptamer-functionalized nano-biosensors. Sensors (Basel) 9(12): 10356-10388, 2009. DOI: 10.3390/s91210356

5 Rabiee N, Chen S, Ahmadi S, Veedu RN: Aptamer-engineered (nano)materials for theranostic applications. Theranostics 13(15): 5183-5206, 2023. DOI: 10.7150/thno.85419

6 Urmi R, Banerjee P, Singh M, Singh R, Chhillar S, Sharma N, Chandra A, Singh N, Qamar I: Revolutionizing biomedicine: Aptamer-based nanomaterials and nanodevices for therapeutic applications. Biotechnol Rep (Amst) 42: e00843, 2024. DOI: 10.1016/j.btre.2024.e00843

7 MacKay S, Wishart D, Xing JZ, Chen J: Developing trends in aptamer-based biosensor devices and their applications. IEEE Trans Biomed Circuits Syst 8(1): 4-14, 2014. DOI: 10.1109/tbcas.2014.2304718

8 Onaş AM, Dascălu C, Raicopol MD, Pilan L: Critical design factors for electrochemical aptasensors based on target-induced conformational changes: the case of small-molecule targets. Biosensors (Basel) 12(10): 816, 2022. DOI: 10.3390/bios12100816

9 Chen T, Shukoor MI, Chen Y, Yuan Q, Zhu Z, Zhao Z, Gulbakan B, Tan W: Aptamer-conjugated nanomaterials for bioanalysis and biotechnology applications. Nanoscale 3(2): 546-556, 2011. DOI: 10.1039/c0nr00646g

10 Zhou J, Rossi J: Aptamers as targeted therapeutics: current potential and challenges. Nat Rev Drug Discov 16(3): 181-202, 2017. DOI: 10.1038/nrd.2016.199

11 Zhou H, Li Y, Wu W: Aptamers: promising reagents in biomedicine application. Adv Biol 8(6): e2300584, 2024. DOI: 10.1002/adbi.202300584

12 Lin K, Gan Y, Zhu P, Li S, Lin C, Yu S, Zhao S, Shi J, Li R, Yuan J: Hollow mesoporous polydopamine nanospheres: synthesis, biocompatibility and drug delivery. Nanotechnol 32(28): 285602, 2021. DOI: 10.1088/1361-6528/abf4a9

13 Zhu M, Shi Y, Shan Y, Guo J, Song X, Wu Y, Wu M, Lu Y, Chen W, Xu X, Tang L: Recent developments in mesoporous polydopamine-derived nanoplatforms for cancer theranostics. J Nanobiotechnology 19(1): 387, 2021. DOI: 10.1186/s12951-021-01131-9
14 Jin A, Wang Y, Lin K, Jiang L: Nanoparticles modified by polydopamine: Working as "drug" carriers. Bioact Mater 5(3): 522-541, 2020. DOI: 10.1016/j.bioactmat.2020.04.003
15 Zandieh M, Hagar BM, Liu J: Interfacing DNA and polydopamine nanoparticles and its applications. Part Part Syst Charact 37(11): 2000208, 2020. DOI: 10.1002/ppsc.202000208
16 Lynge ME, van der Westen R, Postma A, Städler B: Polydopamine—a nature-inspired polymer coating for biomedical science. Nanoscale 3(12): 4916, 2011. DOI: 10.1039/c1nr10969c
17 Lee H, Dellatore SM, Miller WM, Messersmith PB: Mussel-inspired surface chemistry for multifunctional coatings. Science 318(5849): 426-430, 2007. DOI: 10.1126/science.1147241
18 Ryu JH, Messersmith PB, Lee H: Polydopamine surface chemistry: a decade of discovery. ACS Appl Mater Interfaces 10(9): 7523-7540, 2018. DOI: 10.1021/acsami.7b19865
19 Wang C, Zhou J, Wang P, He W, Duan H: Robust nanoparticle–DNA conjugates based on mussel-inspired polydopamine coating for cell imaging and tailored self-assembly. Bioconjug Chem 27(3): 815-823, 2016. DOI: 10.1021/acs.bioconjchem.6b00021
20 Schulz C, Hecht J, Krüger-Genge A, Kratz K, Jung F, Lendlein A: Generating aptamers interacting with polymeric surfaces for biofunctionalization. Macromol Biosci 16(12): 1776-1791, 2016. DOI: 10.1002/mabi.201600319
21 Qiang W, Hu H, Sun L, Li H, Xu D: Aptamer/polydopamine nanospheres nanocomplex for *in situ* molecular sensing in living cells. Anal Chem 87(24): 12190-12196, 2015. DOI: 10.1021/acs.analchem.5b03075
22 Wang K, He MQ, Zhai FH, He RH, Yu YL: A novel electrochemical biosensor based on polyadenine modified aptamer for label-free and ultrasensitive detection of human breast cancer cells. Talanta 166: 87-92, 2017. DOI: 10.1016/j.talanta.2017.01.052
23 Bisht N, Dwivedi N, Khosla A, Mondal DP, Srivastava AK, Dhand C: Review—recent advances in polydopamine-based electrochemical biosensors. J Electrochem Soc 169(10): 107505, 2022. DOI: 10.1149/1945-7111/ac9b95
24 Safari Yazd H, Yang Y, Li L, Yang L, Li X, Pan X, Chen Z, Jiang J, Cui C, Tan W: Precise deposition of polydopamine on cancer cell membrane as artificial receptor for targeted drug delivery. iScience 23(12): 101750, 2020. DOI: 10.1016/j.isci.2020.101750
25 Cohen R, Cohen Y, Mukha D, Yehezkeli O: Oxygen insensitive amperometric glucose biosensor based on FAD dependent glucose dehydrogenase co-entrapped with DCPIP or DCNQ in a polydopamine layer. Electrochim Acta 367: 137477, 2021. DOI: 10.1016/j.electacta.2020.137477
26 Xu L, Chopdat R, Li D, Al-Jamal KT: Development of a simple, sensitive and selective colorimetric aptasensor for the detection of cancer-derived exosomes. Biosens Bioelectron 169: 112576, 2020. DOI: 10.1016/j.bios.2020.112576
27 Bayat P, Nosrati R, Alibolandi M, Rafatpanah H, Abnous K, Khedri M, Ramezani M: SELEX methods on the road to protein targeting with nucleic acid aptamers. Biochimie 154: 132-155, 2018. DOI: 10.1016/j.biochi.2018.09.001
28 Yu Y, Liang C, Lv Q, Li D, Xu X, Liu B, Lu A, Zhang G: Molecular selection, modification and development of therapeutic oligonucleotide aptamers. Int J Mol Sci 17(3): 358, 2016. DOI: 10.3390/ijms17030358
29 Ghosh S, Datta D, Cheema M, Dutta M, Stroscio MA: Aptasensor based optical detection of glycated albumin for diabetes mellitus diagnosis. Nanotechnol 28(43): 435505, 2017. DOI: 10.1088/1361-6528/aa893a
30 Liu J, You M, Pu Y, Liu H, Ye M, Tan W: Recent developments in protein and cell-targeted aptamer selection and applications. Curr Med Chem 18(27): 4117-4125, 2011. DOI: 10.2174/092986711797189619
31 Tao W, Zeng X, Wu J, Zhu X, Yu X, Zhang X, Zhang J, Liu G, Mei L: Polydopamine-based surface modification of novel nanoparticle-aptamer bioconjugates for *in vivo* breast cancer targeting and enhanced therapeutic effects. Theranostics 6(4): 470-484, 2016. DOI: 10.7150/thno.14184
32 Zhang L, Wu J, Xiao M, Zhang S, Ren S, Luo D, Xi F, Liu H, Li Y, Li Q, Jing Y: Aptamer-functionalized gold nanoparticles for fast and selective electrochemical sensing of lead in tobacco. Int J Electrochem Sci 19(12): 100858, 2024. DOI: 10.1016/j.ijoes.2024.100858
33 White RJ, Phares N, Lubin AA, Xiao Y, Plaxco KW: Optimization of electrochemical aptamer-based sensors *via* optimization of probe packing density and surface chemistry. Langmuir 24(18): 10513-10518, 2008. DOI: 10.1021/la800801v
34 Hu Z, Zhu R, Figueroa-Miranda G, Zhou L, Feng L, Offenhäusser A, Mayer D: Truncated electrochemical aptasensor with enhanced antifouling capability for highly sensitive serotonin detection. Biosensors (Basel) 13(9): 881, 2023. DOI: 10.3390/bios13090881
35 Lönne M, Bolten S, Lavrentieva A, Stahl F, Scheper T, Walter JG: Development of an aptamer-based affinity purification method for vascular endothelial growth factor. Biotechnol Rep (Amst) 8: 16-23, 2015. DOI: 10.1016/j.btre.2015.08.006
36 Tian L, Chen C, Gong J, Han Q, Shi Y, Li M, Cheng L, Wang L, Dong B: The convenience of polydopamine in designing SERS biosensors with a sustainable prospect for medical application. Sensors (Basel) 23(10): 4641, 2023. DOI: 10.3390/ s23104641
37 Liu J, Morris MD, Macazo FC, Schoukroun-Barnes LR, White RJ: The current and future role of aptamers in electroanalysis. J Electrochem Soc 161(5): H301-H313, 2014. DOI: 10.1149/2.026405jes
38 Honmane SM, Charde MS, Salunkhe SS, Choudhari PB, Nangare SN: Polydopamine surface-modified nanocarriers

for improved anticancer activity: Current progress and future prospects. OpenNano 7: 100059, 2022. DOI: 10.1016/j.onano.2022.100059
39 Apiwat C, Luksirikul P, Kankla P, Pongprayoon P, Treerattrakoon K, Paiboonsukwong K, Fucharoen S, Dharakul T, Japrung D: Graphene based aptasensor for glycated albumin in diabetes mellitus diagnosis and monitoring. Biosens Bioelectron 82: 140-145, 2016. DOI: 10.1016/j.bios.2016.04.015
40 Akki SU, Werth CJ: Critical Review: DNA aptasensors, are they ready for monitoring organic pollutants in natural and treated water sources? Environ Sci Technol 52(16): 8989-9007, 2018. DOI: 10.1021/acs.est.8b00558
41 Schoukroun-Barnes LR, Macazo FC, Gutierrez B, Lottermoser J, Liu J, White RJ: Reagentless, structure-switching, electrochemical aptamer-based sensors. Annu Rev Anal Chem (Palo Alto Calif) 9(1): 163-181, 2016. DOI: 10.1146/annurev-anchem-071015-041446
42 White RJ, Rowe AA, Plaxco KW: Re-engineering aptamers to support reagentless, self-reporting electrochemical sensors. Analyst 135(3): 589-594, 2010. DOI: 10.1039/b921253a
43 Duan Q, Jia HR, Chen W, Qin C, Zhang K, Jia F, Fu T, Wei Y, Fan M, Wu Q, Tan W: Multivalent aptamer-based lysosome-targeting chimeras (LYTACs) platform for mono- or dual-targeted proteins degradation on cell surface. Adv Sci (Weinh) 11(17): e2308924, 2024. DOI: 10.1002/advs.202308924
44 Aye NNS, Maraming P, Tavichakorntrakool R, Chaibunruang A, Boonsiri P, Daduang S, Teawtrakul N, Prasongdee P, Amornkitbamrung V, Daduang J: A simple graphene functionalized electrochemical aptasensor for the sensitive and selective detection of glycated albumin. Appl Sci 11(21): 10315, 2021. DOI: 10.3390/app112110315
45 Waiwinya W, Putnin T, Pimalai D, Chawjiraphan W, Sathirapongsasuti N, Japrung D: Immobilization-free electrochemical sensor coupled with a graphene-oxide-based aptasensor for glycated albumin detection. Biosensors (Basel) 11(3): 85, 2021. DOI: 10.3390/bios11030085
46 Bunyarataphan S, Dharakul T, Fucharoen S, Paiboonsukwong K, Japrung D: Glycated albumin measurement using an electrochemical aptasensor for screening and monitoring of diabetes mellitus. Electroanalysis 31(11): 2254-2261, 2019. DOI: 10.1002/elan.201900264